Perceived Noise Impact of Transitioning Towards Larger Wind Turbines Using Auralisations

Pockelé, J.S.; Merino Martinez, R.

DOI
10.11581/08042886-dea0-4511-b4bd-6c5403125735

Publication date
2025

Document Version
Final published version

Published in
11th Edition of the International Conferences on Wind Turbine Noise: Conference Proceedings

11th Edition of the

International Conferences on
Wind Turbine Noise

Copenhagen, Denmark – 10th to 13th June 2025

Perceived Noise Impact of Transitioning Towards Larger Wind Turbines Using Auralisations

Josephine Siebert Pockelé[1] and Roberto Merino-Martinez
Delft University of Technology, Faculty of Aerospace Engineering, Kluyverweg 1, 2629HS Delft, the Netherlands

Summary

The human perception of two wind turbines of different sizes, a small NTK turbine and a larger NREL model, was evaluated through their synthetically auralised sound. A wide range of wind speed conditions and observer locations was considered. The simulated sounds were analyzed using equivalent sound pressure levels and psychoacoustic sound quality metrics. Moreover, listening experiments were conducted to evaluate the human response to the same sounds. The least-squares models fitted to the results provided scaling laws for the different sound metrics as a function of wind speed (divided into low- and high-speed regimes) and distance to the observer. At lower wind speeds, the NREL turbine's noise and annoyance levels increase faster with increasing wind speed than the NTK turbine. The results of the NREL turbine at high wind speeds seem to indicate that turbulent boundary layer trailing-edge noise contributes more to annoyance than leading edge turbulent inflow noise. In the listening experiments, the larger wind turbine was perceived roughly 30% more annoying than the smaller one for the same conditions. The equivalent A-weighted sound pressure level and the psychoacoustic annoyance model by Zwicker were reported to closely represent the annoyance ratings reported in the listening experiment.

1. Introduction

Wind turbine noise is an important aspect of planning and permitting of onshore wind farm projects. While offshore turbines offer a compelling alternative, onshore turbines remain the majority of newly installed capacity [1]. The average size of onshore turbines has grown considerably in the last decade. In 2024, the average power rating of newly installed onshore turbines in Europe was 4.6 MW, with the average power of ordered turbines reaching 5.7 MW. Turbines exceeding 10 MW are in development for the onshore wind market at the time of writing [2]. Van den Berg *et al.* [3] showed how this increase in power rating has affected the A-weighted sound levels in a comprehensive study of noise measurements of operating turbines. The study shows little increase in A-weighted noise levels beyond a 2.0-MW rated power while suggesting that recent advances in noise-reduction technologies only affect noise in the 400 – 1600 Hz frequency range [3]. To the best of the authors' knowledge, no studies were found that quantify the effect of increasing size in terms of human sound perception.

Recently, there has been an increased interest in research about the annoyance caused by wind turbine noise, but it usually remains limited to surveys about existing installations [4]–[6]. Typical legislation and

[1]Corresponding author - Email: j.s.pockele@tudelft.nl

research often focus on A-weighted sound pressure levels [7]. Nevertheless, A-weighting is known to have shortcomings in capturing the low-frequency and infrasound content of noise, while this frequency range may, in part, be one of the main causes of wind turbine noise annoyance [8], [9]. Kirkegaard *et al.* [10], [11] indicates the need for tools to enable better community engagement in the planning and mitigation of wind turbine noise.

Auralisation, the creation of sound files from simulated data [12], applied to wind turbine noise modelling, has recently emerged as a possible tool to enable the integration of noise annoyance into the wind turbine design loop [13]–[16]. It furthermore detaches annoyance research from the need for expensive measurement campaigns that were previously required for listening experiments and sound quality assessment. This paper is an application of auralisation to investigate the impact of transitioning to increasingly larger onshore wind turbines on noise perception. A listening experiment campaign was conducted to evaluate the perception of the simulated wind turbine sounds.

Section 2 explains the auralisation method employed in this study to generate the synthetic wind turbine sounds, and section 3 gathers the main inputs for the simulation setup. The analysis methods are briefly described in section 4. The results of the simulations and the listening experiments are gathered in sections 5 and 6, respectively. Lastly, the conclusions are drawn in section 7.

2. Auralisation Method

The method to auralise wind turbine noise in this paper is based on the method described by Pockelé [15]. The main difference is the replacement of the Gaussian beam tracing with a simpler image-source model for the sound propagation.

The wind turbine aeroelastic-aeroacoustic modelling is achieved with the second-generation Horizontal Axis Wind turbine simulation Code (HAWC2), developed by DTU (Technical University of Denmark) [17], [18]. The aero-noise module of HAWC2 accounts for three aerodynamic noise generation mechanisms: turbulent boundary layer trailing-edge noise (TE), turbulent inflow leading-edge noise (TI), and stall noise. In HAWC2, TE noise is modelled using the modified TNO model [19] by Bertagnolio *et al.* [20], TI noise is modelled using Amiet's theory [21], and stall noise is accounted for with the model by Bertagnolio *et al.* [22]. The aero-noise module is used to estimate the power spectral density spectrograms at the one-third-octave band central frequencies and at the selected observer locations.

Since HAWC2 only accounts for spreading losses and the Doppler effect [18], additional corrections are applied to account for ground reflections and atmospheric absorption. The received sound is only available per blade or for the full wind turbine. Hence, the corrections are applied assuming a single monopole sound source at 85 percent of each blade's span. Before applying these corrections, the HAWC2 output spectrograms are linearly interpolated to narrow-band frequencies, to match the required number of samples in the Inverse Short-Time Fourier Transform (ISTFT).

Ground effects are modelled using the approach by Embleton *et al.* [23], together with the ground impedance model by Delany and Bazley [24]. The direct and reflected spectrograms are separated at this stage to account for the difference in propagation distance when applying the atmospheric absorption. Both spectrograms are given an equal random phase, and the reflected one is supplemented with the frequency-dependent phase differences calculated in the ground reflection model. One limitation of the monopole point source assumption is the overestimation of the interference between the direct and reflected noise. In reality, the blade acts as a distributed noise source, where noise emitted from different radial positions will have different interference patterns, which results in little to no spectral dips in the measured sound on the ground [25]. In the measured spectra in [17], no clear interference patterns can be distinguished, confirming this as a modelling limitation of this method.

The noise attenuation due to atmospheric absorption is accounted for using the model in ISO standard 9613-1 by Bass *et al.* [26], [27]. A constant, frequency-dependent set of absorption coefficients $\alpha(f)$ is assumed for all propagation paths. Similar to the ground reflections, these are calculated for the interpolated spectrogram frequencies. The attenuation spectra are then applied per blade and separately for the direct and reflected propagation paths.

Finally, the six spectrograms (for each blade: one for the direct and one for the reflected sound signal) are reconstructed into separate sound signals using the ISTFT, which are added together into the final auralised noise signal. In the ISTFT, a Hanning window is applied to smooth the transition between hops. To obtain a signal with the desired sampling frequency f_s, the spectrograms have been interpolated in the frequency domain, so they comply with the following requirement on the number of samples N_{hop} in a single STFT hop length:

$$N_{\text{hop}} = f_s \cdot \Delta t_{\text{STFT}} + 1 \tag{1}$$

where Δt_{STFT} is the time step of the spectrogram. For this paper, a reconstruction overlap of 50% is set, which means that the requirement becomes:

$$N_{f,\text{required}} = 2N_{\text{hop}} \tag{2}$$

3. Simulation Setup

3.1 Wind Turbine Simulation Models

For this work, two HAWC2 simulation models were used: (1) the *NREL 5MW reference wind turbine* (NREL)[1], and (2) the *Nordtank NTK 500/41* (NTK) wind turbine [28]. The NREL wind turbine was selected to represent the size, power rating, and control mechanism of modern onshore wind turbines since it is the only simulation model of this size, which is readily available to the authors. The NTK turbine, on the other hand, was chosen to represent older and smaller wind turbines. The size of both turbines is compared in Figure 1, while some other relevant specifications are compared in Table 1.

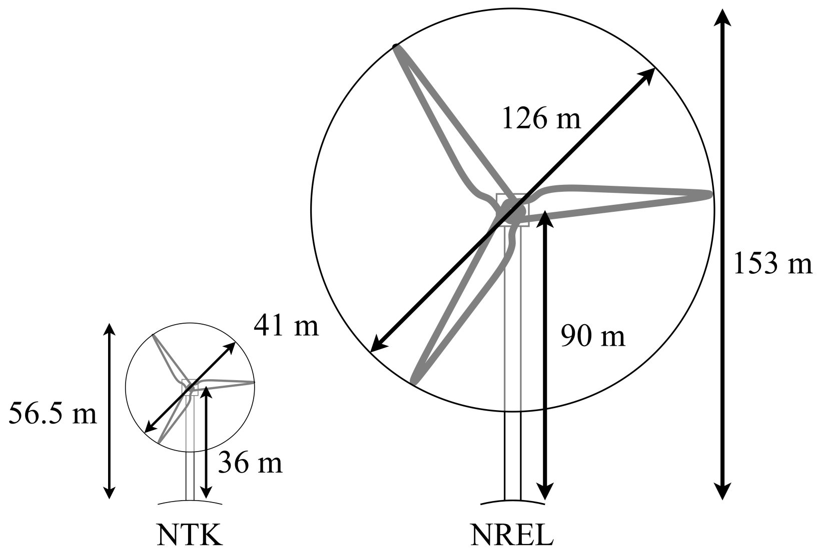

Figure 1 Size comparison of the NTK and NREL wind turbine models used in this work.

[1]Available online: `https://gitlab.windenergy.dtu.dk/hawc-reference-models`

Table 1 Relevant specifications of the NREL and the NTK wind turbines.

	NTK [29]	NREL [30]
Power Rating, [MW]	0.5	5.0
Control	Passive	Active
Mechanism	Aerodynamic Stall	Collective Pitch
Rotor Speed, [rpm]	Constant (27.1)	Variable (6.9 - 12.1)

For aeroacoustic calculations in HAWC2, tabulated airfoil boundary layer parameters are required [18]. In the dataset by Bertagnolio *et al.* [28], multiple such tables are available for the NTK wind turbine. To allow for parity between both turbines, the XFoil results table with the critical amplification parameter $N_{\text{crit}} = 3$ is used. For the NREL turbine, this table is established using XFoil simulations [31], using the publicly available blade and airfoil geometries[2]. The range of Reynolds numbers and angles of attack in this boundary layer table were determined based on the local relative inflow velocity and angle of attack, found through a series of verification simulations. The N_{crit} parameter in XFoil was set to 3, while the boundary layer was tripped at 10% of the chord length.

3.2 Simulated Operational Conditions

The auralisations were conducted under a set of common atmospheric conditions. The air temperature, pressure, and density were set to 15°C, 1013.25 hPa, and 1.225 kg/m^3, respectively, based on the ground level conditions in the ISO 2533:1975 standard atmosphere [32]. The relative humidity of the air was set to 80%, based on the average air humidity in the Netherlands from the last 30 years [33]. The inflow turbulence intensity was set to 10%.

Simulations were performed for a range of wind speeds from 5.0 m/s to 25.0 m/s, in steps of 5.0 m/s. The cut-in speed of both turbines, 4.0 m/s, as well as the NREL turbine's rated wind speed, 11.4 m/s, were also simulated. Virtual microphone positions were defined upstream and downstream of the turbines, at 153 m, 500 m, 1000 m, and 2000 m, where the first distance represents the standardised measurement distance of the NREL wind turbine [34].

Pockelé and Merino-Martinez [35] showed an unfavourable relation between adding background noise and loudness-based sound quality metric results. Therefore, no ambient noise is considered, such that only the effects of the wind turbine noise are evaluated.

4. Analysis Methods

4.1 Sound Quality Metrics

Sound Quality Metrics (SQMs) describe the subjective perception of sound by human hearing, unlike the L_p metric, which quantifies the purely physical magnitude of sound based on pressure fluctuations. Previous studies [13], [36] showed that these metrics better capture the auditory behavior of the human ear compared to conventional sound metrics typically employed in noise evaluations. The four most commonly used SQMs [37] are:

- Loudness (N): Subjective perception of sound magnitude corresponding to the overall sound intensity [38]. The loudness results in this paper are expressed in loudness levels L_N in phon.
- Sharpness (S): Representation of the high-frequency sound content [39].
- Roughness (R): Hearing sensation caused by sounds with modulation frequencies between 15 Hz and

[2]Airfoil geometries provided by Nando Timmer, available online: `https://forums.nrel.gov/uploads/short-url/t5k5D4TrCNECxJJ7vwFKEeqaBoi.xls`

300 Hz [40].
- Fluctuation strength (FS): Assessment of slow fluctuations in loudness with modulation frequencies up to 20 Hz, with maximum sensitivity for modulation frequencies around 4 Hz [41].

These SQMs were calculated for each wind turbine noise sample. The 5% percentile values of each metric (i.e., the value of each SQM exceeded 5% of the total recording time) were combined into a global psychoacoustic annoyance (PA) metric following the model outlined by Zwicker [42]. All SQMs and the PA metric were calculated using the open-source MATLAB Sound Quality Analysis Toolbox (SQAT) v1.2 [37], [43], which is available on GitHub[3].

4.2 Least-Squares Modelling

To allow for a more intuitive understanding of the results, least-squares models were fitted to the simulation outputs. As a baseline, the sound pressure levels and SQMs were related to the average wind speed (U_∞), and the distance up- and downstream (r). An interaction term between wind speed and distance was also tested for all metrics. Based on the findings of van den Berg *et al.* [3], a logarithmic relation with wind speed is assumed, while the distance term is also made logarithmic to match the general spherical spreading trend. The baseline least-squares model is described by Equation 3:

$$\text{metric} = x_1 \cdot \log_{10}\left(\frac{U_\infty}{11.4}\right) + x_2 \cdot \log_{10}\left(\frac{r}{153}\right) + x_3 \cdot \log_{10}\left(\frac{U_\infty}{11.4}\right) \cdot \log_{10}(r) + x_4 \tag{3}$$

The NREL wind turbine has two distinct modes of operation: (1) variable speed, constant pitch for low wind speeds ($U_\infty < 11.4$ m/s), and (2) constant speed, variable pitch for high wind speeds ($U_\infty > 11.4$ m/s). Similarly, the NTK wind turbine experiences partial blade aerodynamic stall at higher wind speeds. Therefore, the models were fitted separately for data where $U_\infty \leq 11.4$ m/s, and where $U_\infty \geq 11.4$ m/s. For the NREL wind turbine, the initial data analysis showed significant differences for the upstream and downstream directions in the high-wind-speed regime. Therefore, the NREL turbine results, at mean wind speeds above 11.4 m/s, are fitted to separate models for each propagation direction.

5. Simulation Results

5.1 Equivalent Sound Pressure Levels

As a baseline, the unweighted equivalent sound pressure levels $L_{p,eq}$ of the auralisations are analysed. Figure 2 presents the results for both wind turbines, side by side. The first notable difference is the wind speed slopes in the low-wind-speed region. The NREL turbine's noise levels grow considerably faster with increasing wind speed compared to the NTK turbine. In the high-wind speed regime, both turbines show a very similar increase in noise levels with wind speed. As expected, the logarithmic decrease of noise level with distance fits well to the data. For the NREL turbine, no large differences are observed between the upstream and downstream directions at high wind speeds.

The coefficients of the least-squares models are presented in Table 2 and Table 3 for the low- and high-wind speed regimes, respectively. The cross-term with wind speed and distance has been removed from the model, as this resulted in high p-values and lower adjusted R^2 values.

[3]Available online: `https://github.com/ggrecow/sqat`

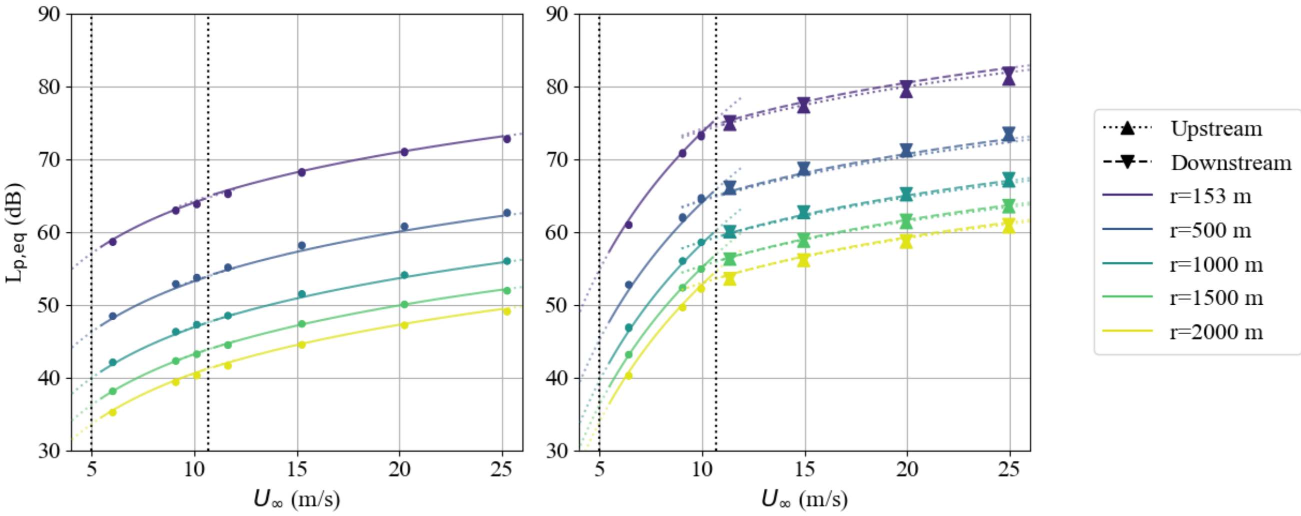

(a) NTK wind turbine. *(b) NREL wind turbine.*

Figure 2 Equivalent sound pressure levels of the auralisations and the least-squares model curves.

The relation with distance has, as expected, a coefficient close to −20, which corresponds to a sound power decrease with $\frac{1}{r^2}$. The differences from −20 can be explained by the ground reflections and atmospheric absorption. Because of the normalisation to $U_\infty = 11.4$ m/s and $r = 153$ m, the intercepts show the predicted sound pressure levels at this wind speed and distance. The NREL wind turbine is considerably louder, with an approximate $L_{p,eq}$ difference of 10 dB over the NTK turbine.

The initial observations of the relation with wind speed are confirmed by the wind speed slope coefficient. Interestingly, neither turbine shows the expected $50 \log(U_\infty)$ relation reported by van den Berg et al. [3]. The similar slope between both turbines in the high-wind-speed region can be explained by both turbines operating at a constant RPM. This is further supported by the slope of the NTK turbine not changing significantly between both regimes. The higher slope of the NREL turbine in the low-wind-speed regime can be explained by the significant increase of local flow velocity over the blades with increasing rotor RPM. The increase of 5.2 RPM from the minimum to the maximum RPM of the NREL turbine results in a local flow velocity increase of 34 m/s at the blade tip ($R_{blade} = 63$ m).

Table 2 Least-squares fit coefficients for $L_{p,eq}$ at low wind speeds ($U_\infty < 11.4$). All p-values are $\ll 0.05$.

	$\log_{10}(U_\infty)$	$\log_{10}(r)$	Intercept	Adjusted R^2
NTK	23.168	−21.000	65.323	0.999
NREL	62.667	−18.726	77.219	0.997

Table 3 Least-squares fit coefficients for $L_{p,eq}$ at high wind speeds ($U_\infty \geq 11.4$). All p-values are $\ll 0.05$.

	$\log_{10}(U_\infty)$	$\log_{10}(r)$	Intercept	Adjusted R^2
NTK	22.250	−21.232	65.505	0.998
NREL (upstream)	20.307	−18.671	74.983	0.995
NREL (downstream)	21.018	−18.996	75.338	0.997

5.2 A-weighted Equivalent Sound Pressure Levels

The plots of the A-weighted equivalent sound pressure levels $L_{A,eq}$ in Figure 3 show some similarities but also some major differences to the unweighted levels presented in Figure 2. In the low-wind-speed regime, the slopes with wind speed show a similar trend as the unweighted levels, with the levels of the NREL turbine increasing significantly faster than the NTK turbine. At higher wind speeds, the main difference with the unweighted levels is found for the NREL turbine. Downstream of the turbine, the A-weighted levels remain relatively constant with wind speed, whereas the upstream levels decrease. This difference between the A-weighted and unweighted levels indicates a possible change of the dominant noise generation mechanism towards lower-frequency noise.

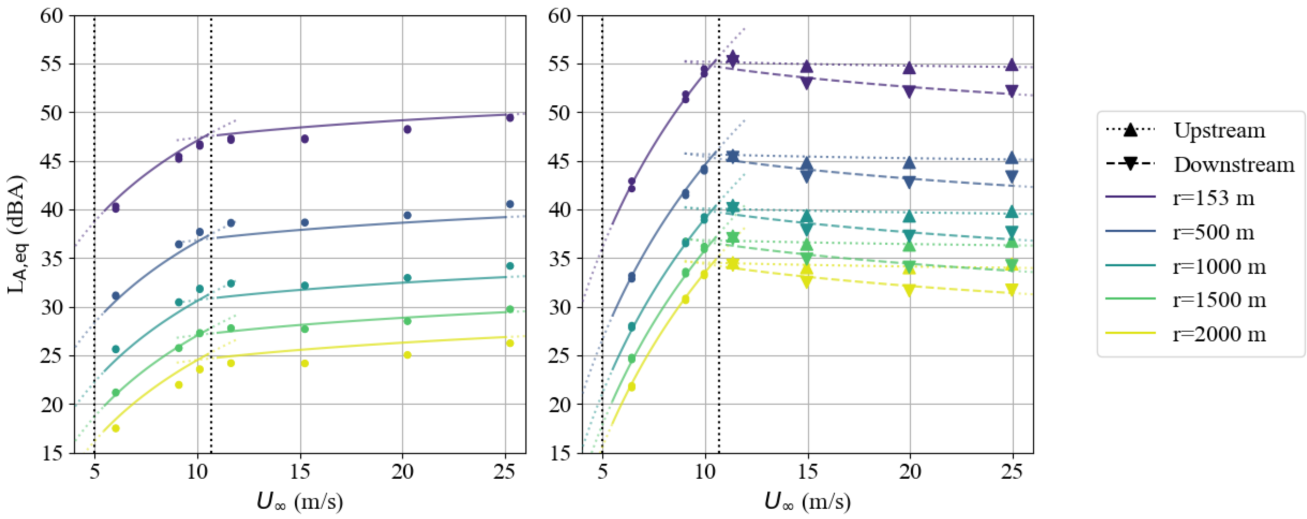

(a) NTK wind turbine. *(b) NREL wind turbine.*

Figure 3 A-weighted equivalent sound pressure levels of the auralisations and the least-squares model curves.

Table 4 Least squares fit coefficients for $L_{A,eq}$ at low wind speeds ($U_\infty < 11.4$). All p-values are $\ll 0.05$.

	$\log_{10}(U_\infty)$	$\log_{10}(r)$	Intercept	Adjusted R^2
NTK	27.682	−20.215	48.642	0.989
NREL	59.613	−18.360	57.412	0.999

Table 5 Least squares fit coefficients for $L_{A,eq}$ at high wind speeds ($U_\infty \geq 11.4$). All p-values are $\ll 0.05$.

	$\log_{10}(U_\infty)$	$\log_{10}(r)$	Intercept	Adjusted R^2
NTK	5.923	−20.480	47.711	0.987
NREL (upstream)	−1.362	−18.495	55.102	0.997
NREL (downstream)	−7.531	−18.325	54.417	0.993

Observing the coefficients of the least-squares model fits in Table 4 and Table 5 confirms the above-noted changes. Additionally, the NTK turbine shows a decreased relation with wind speed in the high-speed regime, which creates a more distinct transition between the low- and high-wind-speed regimes than for $L_{p,eq}$. This again shows a change in the dominant noise generation mechanism when compared against the unweighted equivalent level results. Regarding the intercepts, A-weighting decreases the equivalent levels by approximately 20 dB compared to the unweighted sound pressure levels.

5.3 Loudness Level

The first psychoacoustic SQM results are those regarding the mean loudness level, $L_{N,mean}$. During the preliminary analysis, the cross-term coefficient x_3 of the least-squares model in Equation 3 was found to be highly significant, whereas the wind speed coefficient x_1 had a p-value > 0.05. Therefore, the loudness level is fitted to the least-squares model without the x_1 term. This indicates a strong combined effect of wind speed and distance in human loudness perception.

From Figure 4, similar trends are derived compared to the A-weighted levels. In the low-wind-speed region, the loudness of the NREL turbine increases more rapidly with wind speed compared to the NTK turbine. At high wind speeds, there is once more a clear division between the upstream and downstream propagation for the NREL turbine. Visually, the loudness levels of both turbines show a closer agreement than the $L_{A,eq}$.

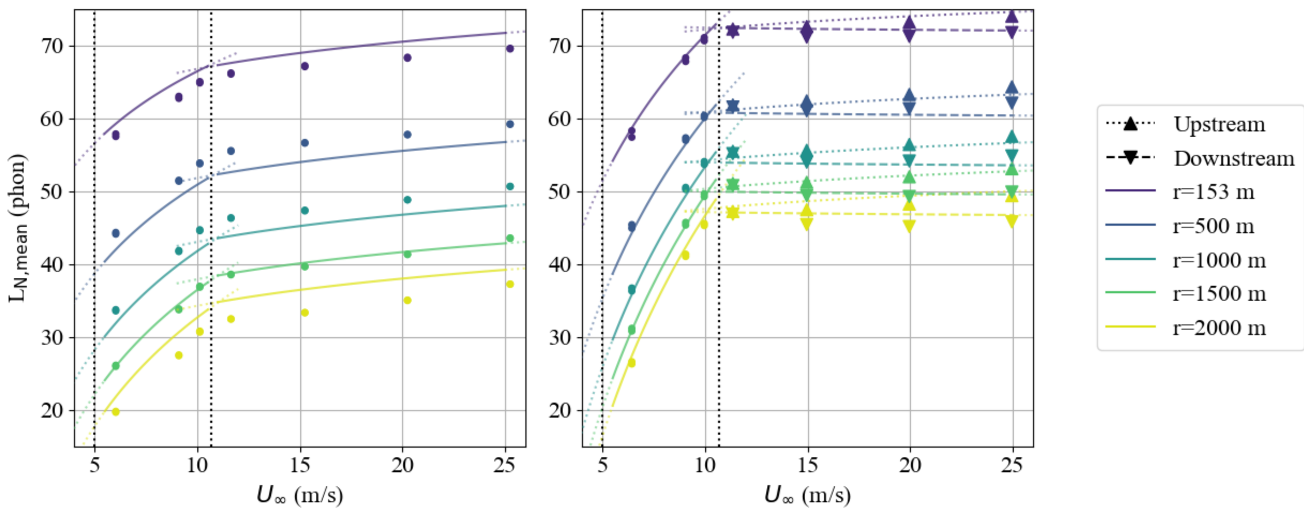

(a) *NTK wind turbine.* (b) *NREL wind turbine.*

Figure 4 Mean loudness level of the auralisation results and the least-squares model curves.

The latter observation is confirmed in Table 6 and Table 7, where the intercepts are relatively closer together than those for the A-weighted levels. On the other hand, both turbines show a different relation with distance to the observer. It should be noted, based on the plots in Figure 4, that the distance fit for the NTK turbine is not as good as for the NREL turbine. The observation remains valid, however, as the data shows a larger level decrease than the model coefficient implies. One implication of this observation is that modern turbines may require larger distances to obtain an equivalent decrease in perceived loudness compared to older turbines.

Table 6 Least squares fit coefficients for $L_{n,mean}$ for low wind speeds ($U_\infty < 11.4$). All p-values are $\ll 0.05$.

	$\log_{10}(U_\infty) \times \log_{10}(r)$	$\log_{10}(r)$	Intercept	Adjusted R^2
NTK	15.009	−29.409	68.282	0.976
NREL	30.409	−20.451	75.160	0.996

Table 7 *Least squares fit coefficients for $L_{n,mean}$ for high wind speeds ($U_\infty \geq 11.4$). All p-values are $\ll 0.05$, except for underlined coefficient.*

	$\log_{10}(U_\infty) \times \log_{10}(r)$	$\log_{10}(r)$	Intercept	Adjusted R^2
NTK	12.408	−29.114	67.455	0.965
NREL (upstream)	6.052	−22.048	72.501	0.993
NREL (downstream)	$\underline{-1.011}$	−22.676	72.366	0.988

5.4 Psychoacoustic Annoyance

For the psychoacoustic annoyance (PA) metric, the least-squares model is fit to the mean values as $10 \cdot \log_{10}(10 \cdot \mathrm{PA_{mean}})$, since the relation with annoyance ratings in listening experiments is generally found to be logarithmic [36], [44]. The preliminary analysis also found a better adjusted R^2 when using the logarithm of $\mathrm{PA_{mean}}$. Figure 5 shows a similar relation with wind speed and distance compared to the loudness levels. In previous work, loudness was found to be the primary contributing factor to the annoyance from wind turbine noise [45].

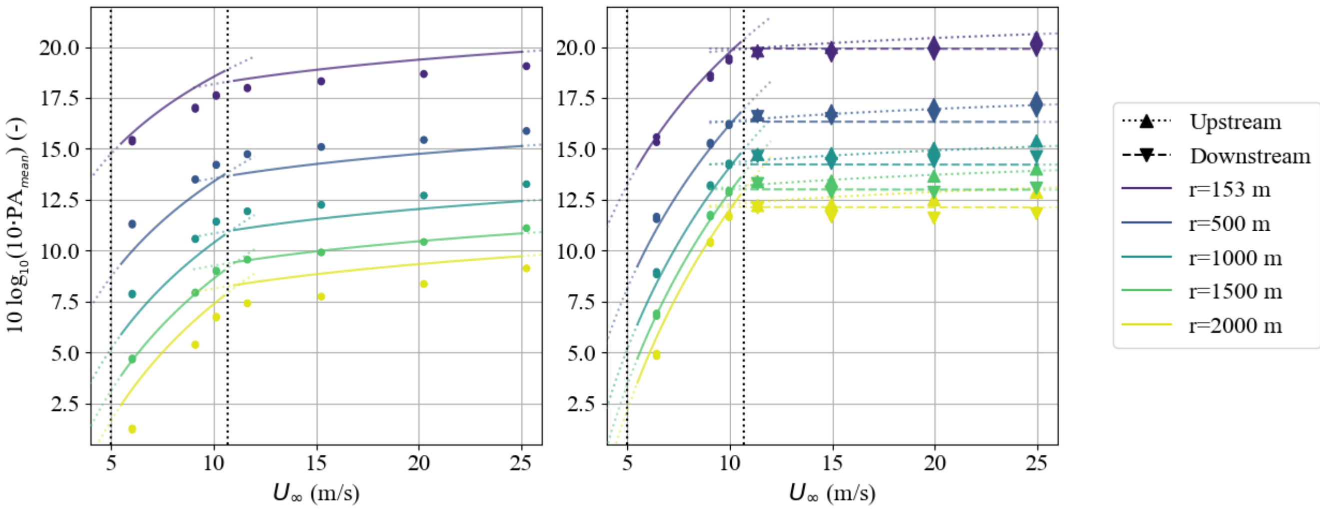

(a) NTK wind turbine. *(b) NREL wind turbine.*

Figure 5 *Mean Psychoacoustic Annoyance (PA) of the auralisation results and the least-squares model curves.*

The main finding in Table 8 and Table 9 is the very similar intercepts between both turbines. Combined with the wind speed and distance relations, it can be derived that the NREL turbine is only expected to be more annoying at low wind speeds or at long distances. This is also visible in Figure 5. The main point of interest is the difference between up- and downstream PA values at high wind speeds for the NREL turbine. This finding does not line up well with the survey findings by Müller *et al.* [6], who reported higher annoyance downstream of a wind farm.

Table 8 *Least squares fit coefficients for $10 \cdot \log_{10}(10 \cdot PA_{mean})$ at low wind speeds ($U_\infty < 11.4$). All p-values are $\ll 0.05$.*

	$\log_{10}(U_\infty) \times \log_{10}(r)$	$\log_{10}(r)$	Intercept	Adjusted R^2
NTK	5.760	−9.675	19.251	0.951
NREL	9.916	−6.363	20.983	0.991

Table 9 *Least squares fit coefficients for $10 \cdot \log_{10}(10 \cdot PA_{mean})$ at high wind speeds ($U_\infty \geq 11.4$). All p-values are $\ll 0.05$, except for underlined coefficient.*

	$\log_{10}(U_\infty) \times \log_{10}(r)$	$\log_{10}(r)$	Intercept	Adjusted R^2
NTK	3.986	−8.995	18.404	0.961
NREL (upstream)	1.988	−6.774	19.957	0.993
NREL (downstream)	<u>−0.046</u>	−6.975	19.924	0.987

5.5 Low-Frequency Noise Content

Because of the previously discussed differences between the unweighted and A-weighted sound pressure levels, the low-frequency content of the wind turbine noise emissions is also investigated. For this purpose, the difference between the C- and A-weighted equivalent sound pressure levels ($L_{C,eq} - L_{A,eq}$) is used, based on the work by Vos and Houben [46]. In the preliminary analysis, the least-squares model in Equation 3 is found not to represent the data well. Therefore, based on the scatter plot in Figure 6, the second-degree polynomial in Equation 4 is fit to the data instead.

$$L_{C,eq} - L_{A,eq} = x_1 \cdot (U_\infty - 11.4)^2 + x_2 \cdot (U_\infty - 11.4) + x_3 \cdot \left(\frac{r}{153}\right)^2 + x_4 \cdot \left(\frac{r}{153}\right) + x_5 \tag{4}$$

In general, the low-frequency content of the noise emissions increases with the wind speed for all distances. A dip in low-frequency noise around 11.4 m/s is observed in Figure 6, as well as large differences between upstream and downstream for the NREL turbine at high wind speeds. In the low-wind-speed regime and upstream, both turbines show a similar trend between low-frequency noise and wind speed.

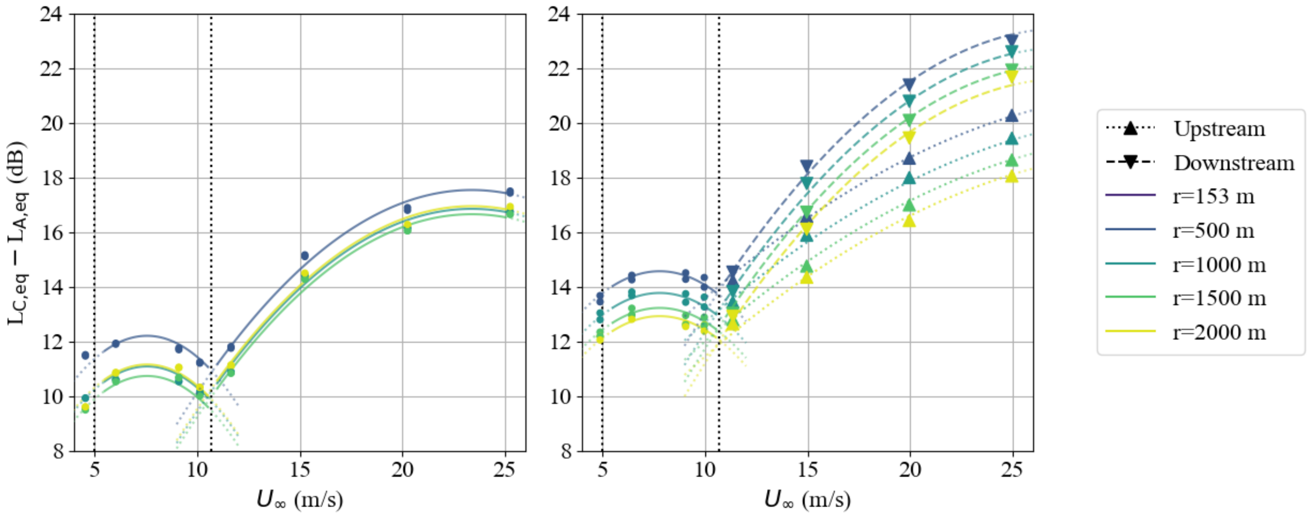

(a) NTK wind turbine. *(b) NREL wind turbine.*

Figure 6 *Difference between C- and A-weighted sound pressure levels of the auralisation results, as a measure of low frequency noise content, and the least-squares model curves.*

Remarkably, the low-frequency trends of the NREL turbine match the surveyed descriptions of typical situations of wind turbine noise annoyance by Müller *et al.* [6, Sec. 3.4.3]. Their survey participants mostly describe high-wind-speed conditions and conditions where they are downstream from the turbine as situations of wind turbine noise annoyance. Given that low-frequency noise propagates better through walls and windows [47], this could partially explain annoyance in indoor situations.

Given that leading-edge turbulent-inflow (TI) noise contributes most to the low-frequency noise of wind turbines, the NREL turbine results seem to imply that a greater amount of TI noise is emitted in the downstream direction compared to upstream. With $L_{A,eq}$ showing the opposite trend, the turbulent boundary layer trailing-edge (TE) noise seems to propagate more upstream than downstream. Since the PA metric also shows larger values in the upstream direction for the NREL turbine, this implies that the TE noise of modern turbines contributes more to the annoyance than the TI noise, as expected from literature [48].

6. Listening Experiment

To validate the numerical results with human perception, a listening experiment was conducted in the Psychoacoustic Listening Laboratory (PALILA) at the Delft University of Technology [49]. This experiment combined multiple studies regarding wind turbine noise. Only the part relevant to this paper is presented.

6.1 Experimental Setup

PALILA is a box-in-box, soundproof booth with a floor plan of 2.32 m × 2.32 m, and a height of 2.04 m. The walls, floor, and ceiling are built with a modular sandwich structure of two 19 mm fibreglass panels with a 52 mm polyurethane foam core. The door is made from the same material and is acoustically sealed. The booth is connected to the floor via a vibration-damping system, and the cavity is filled with sound-absorbing foam. The walls are lined with A-B-C-D level acoustic absorbing foam to minimise reflection. Two bass traps are positioned in diagonally opposing corners to minimise low-frequency noise inside the facility. This setup provides a 0.07 s reverberation time and free-field sound propagation for frequencies higher or equal to 1600 Hz. Moreover, the facility is highly isolated from any other external influence, with a transmission loss of 45 dB and an A-weighted background noise level of only 13.4 dBA [49].

The sound reproduction equipment consists of a *Dell Latitude 7340* touchscreen-equipped laptop connected to a pair of *Sennheiser HD560s* open-back headphones. This equipment is calibrated up to 10 kHz, using a *G.R.A.S. 45BB-14 KEMAR* head-and-torso simulator with *G.R.A.S. KB5000 / KB50001 Anthropometric Pinnae*[4]. The reproduction system is accompanied by an open-source, Python-based Graphical User Interface (GUI) [50], which allows for this experiment to be self-guided and self-paced.

After a briefing by the responsible researchers, participants started the experiment with a questionnaire about their age, gender, employment, and education, as well as questions regarding their hearing health and state of well-being. This information is mainly used for reporting statistics and for bias and outlier detection. After answering these questions, participants proceeded to listen to the sound samples and were asked for each sample: "*What number from 0 to 10 best describes how much you are bothered, disturbed or annoyed by the presented noise?*" using an 11-point ICBEN scale. Every seven sound samples, participants are given a mandatory break from listening to alleviate fatigue.

6.2 Sample Selection

From the simulated sounds described in section 3, a subset was selected for testing in the listening experiment. To limit participant fatigue, the number of tested conditions is reduced compared to the numerical results.

Firstly, wind speed is covered by samples at simulated mean wind speeds of 5, 11.4, and 20 m/s. This wind speed range is only tested at a 153 m observer distance, upstream and downstream, and for both wind turbines. This part of the selection resulted in twelve samples. Eight additional samples are used to cover multiple distances from the wind turbine: 153, 500, and 2000 m, all simulated at a mean wind speed of 11.4 m/s. The reproduction time of all samples is limited to 20 s, as a compromise between exposure time and duration of the total experiment.

[4]Full description of the HATS available online: `https://www.grasacoustics.com/products/head-torso-simulators-kemar/kemar-for-ear-headphone-test-2-ch/product/793-gras-45bb-14`

6.3 Population Sample Statistics

Most of the participants in the experiment are a convenience sample from the Delft University of Technology, Faculty of Aerospace Engineering. The experiment had a total of 35 participants. Most participants are not directly related to research about wind turbine noise, decreasing the possibility of bias by experience.

The sample is diverse with 18 men and 17 women, with an average age of 31 years and an 8 year standard deviation. As expected from the recruitment method, most participants are employed for wages, or students, and 29 were employees or students at the university. The self-rated hearing health of the participants was generally good, with 2 "*excellent*", 15 "*very good*", 15 "*good*", and only 2 "*fair*" ratings. The only reported hearing problems were tinnitus (7 participants), or mild colds (2 participants). Furthermore, two participants indicated having had an accident affecting their hearing, and one participant reported being very tired. None of these reported hearing problems resulted in outlier values of the inter-participant cross-correlation presented in Figure 7b.

Figure 7a shows the mean annoyance rating R_{mean} has converged to $3\sigma < 0.5$, meaning the 99.7% confidence interval has converged to within the measurement error of the 11-point annoyance scale. While small, the sample size is thus considered representative of a similar population. Figure 7b shows a high level of inter-participant cross-correlation, with a mean Pearson correlation coefficient $\rho_{x,y} = 0.766$, and no significant outliers.

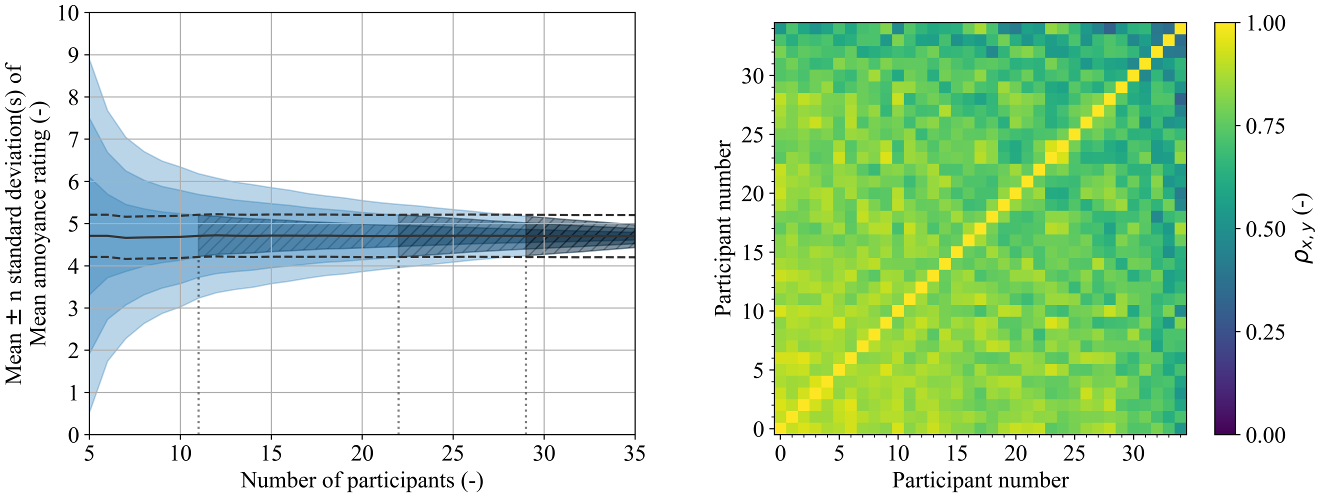

(a) Monte-Carlo convergence of the annoyance ratings. Dashed lines indicate mean annoyance rating ±0.5.

(b) Inter-participant Pearson cross-correlations of the annoyance ratings.

Figure 7 Population sample analysis of the results.

To test for possible gender bias in the results, the best linear unbiased estimate of the ratio between the male and female average annoyance ratings is determined. The estimated $\hat{\frac{R_m}{R_w}} = 0.94 \pm 0.12$ indicates some gender bias. Nevertheless, the p-value of $\frac{R_m}{R_w} \neq 1$, is 0.302, indicating this bias is not statistically significant.

6.4 Listening Experiment Results

In a similar fashion to the numerical metrics, the annoyance ratings for each wind turbine were related to wind speed and distance using a least-squares model. Since the sample selection only tests the distance effect at one wind speed, the cross-term in Equation 3 is omitted, and the mean annoyance ratings are fitted to Equation 5. Similarly to the numerical results, this model is fitted separately for the low- and high-wind-speed regimes and separately for the upstream and downstream results of the NREL turbine in the high-speed region.

$$R_{mean} = x_1 \cdot \log_{10}\left(\frac{U_\infty}{11.4}\right) + x_2 \cdot \log_{10}\left(\frac{U_\infty}{153}\right) + x_3 \tag{5}$$

The results are shown in Figure 8. These plots clearly reflect the difference between both turbines in the low-wind-speed region, showing a larger annoyance increase with wind speed for the NREL compared to the NTK turbine. The difference between the up- and downstream annoyance for the NREL turbine is also clearly reflected. This difference does not look limited to the high-speed regime, however, indicating a deviation from the PA model. Another observation is the relatively high annoyance at a 500-m distance for the NTK turbine compared to the modelled expectation. The potential reason for the latter observation remains unclear since these noise samples are not marked as outliers in the numerical results.

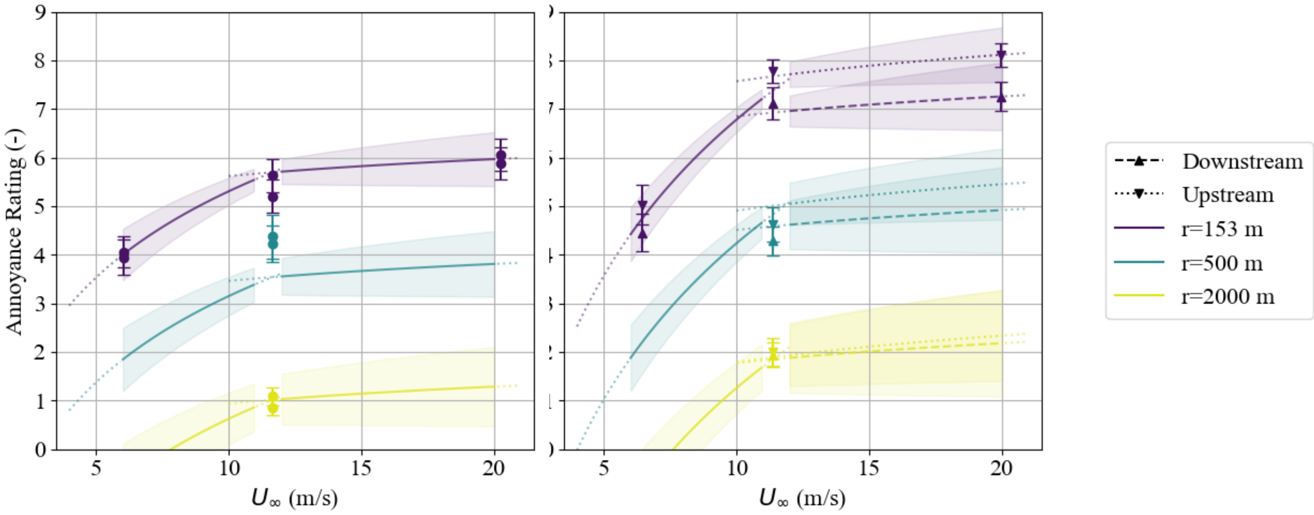

(a) NTK wind turbine. *(b) NREL wind turbine.*

Figure 8 Listening experiment mean annoyance ratings and their standard errors, and least-squares fit curves for the NTK (left) and NREL (right) wind turbines. Shaded areas indicate the confidence intervals of the least-squares models.

The model coefficients in Table 10 and Table 11 immediately highlight the larger annoyance increase with wind speed of the NREL turbine in the low-wind-speed regime. Interestingly, both turbines show a very similar, barely significant (p-values ≈ 0.05) relation with wind speed in the high-speed region. This is different from all numerical results, where the NTK turbine generally showed a stronger relation with wind speed than the NREL turbine, except for the unweighted sound pressure levels.

Table 10 Least squares fit coefficients for the mean annoyance ratings at low wind speeds ($U_\infty < 11.4$). All p-values are $\ll 0.05$.

	$\log_{10}(U_\infty)$	$\log_{10}(r)$	Intercept	Adjusted R^2
NTK	5.910	−4.194	5.641	0.907
NREL	10.693	−4.948	7.387	0.965

Table 11 Least squares fit coefficients for the mean annoyance ratings at high wind speeds ($U_\infty \geq 11.4$). All p-values are $\ll 0.05$, except for underlined coefficients.

	$\log_{10}(U_\infty)$	$\log_{10}(r)$	Intercept	Adjusted R^2
NTK	<u>1.159</u>	−4.194	5.685	0.932
NREL (upstream)	<u>1.817</u>	−5.178	7.672	0.980
NREL (downstream)	<u>1.358</u>	−4.549	6.927	0.979

The coefficients of the distance term, contrary to all numerical results, are of larger magnitude for the NREL compared to the NTK turbine. Thus, the slower decrease in noise and annoyance that was found for the PA metric is not reflected in the listening experiment.

Unlike the numerical PA metric, the intercept values of the measured annoyance ratings show significant differences between both turbines, which correspond closer to the loudness levels and the equivalent A-weighted sound pressure levels.

Similar to the PA metric and $L_{A,eq}$, at high wind speeds, the NREL wind turbine noise is more annoying upstream than downstream. This fact seems to once more support the argument that TE noise contributes more to annoyance than TI noise. While the annoyance ratings are slightly different up- and downstream at low wind speed, the overlap in standard error implies this difference is not very significant.

6.5 Correlation Between Annoyance Ratings and Sound Metrics

Lastly, the correlations between the annoyance ratings from the listening experiment and the logarithm of the mean PA metric and to $L_{A,eq}$ were evaluated, see Figure 9. A logarithmic relation was used to correlate PA since this was found to offer better fits [36], [44]. The coefficients of determination R^2 obtained in both cases are very high, with values higher than 0.95, in general. Overall, the PA metric provides marginally better fits than the $L_{A,eq}$ for both wind turbines considered.

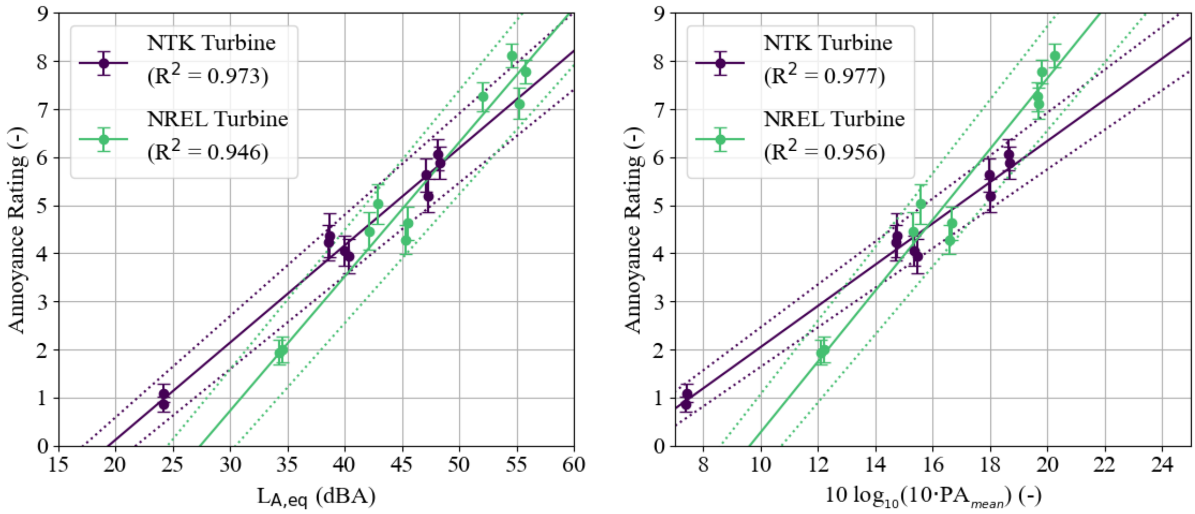

Figure 9 Correlation between the mean annoyance ratings reported in the listening experiments and $L_{A,eq}$ (left) and PA (right, in logarithmic scale). Data points show the mean annoyance ratings and their standard errors. The dotted lines show the standard errors of the Least-Squares fit curves.

On the other hand, Figure 9 shows the annoyance ratings relate differently to the noise metrics for each turbine. This shows that neither metric captures the full variability of the experienced annoyance by both turbines. Merino-Martinez *et al.* [36] commented that this relation can differ depending on the noise source and conditions under investigation. Hence, this result was not unexpected but rather interesting.

7. Conclusion

This paper investigated the variation in noise perception of wind turbines caused by transitioning towards larger wind turbines. Synthetic sound samples were auralised for two different wind turbines using a simulation-based method. A 500 kW, 41 m diameter, stall-controlled Nordtank NTK500/41 wind turbine was used to represent small, older onshore wind turbines. The NREL 5 MW reference wind turbine, with a 126 m, pitch-controlled variable speed rotor, was used to represent modern, large onshore turbines.

Results were presented in sound pressure levels, sound quality metrics (SQMs), and listening experiment annoyance ratings. All metrics show that the noise of the NREL wind turbine in the low-wind-speed regime ($U_\infty < 11.4$ m/s) has a stronger increase in noise and annoyance levels with wind speed than the NTK turbine. Based on the unweighted sound pressure level results, this is expected to be due to the variable rotor speed of the NREL turbine compared to the constant rotor speed of the NTK turbine.

In the high-wind-speed region ($U_\infty > 11.4$ m/s), the NREL turbine exhibits differences between the up- and downstream direction, unlike the NTK turbine. From the analysis of the low frequency noise content, in terms of $L_{A,eq} - L_{C,eq}$, the differences between the propagation directions seem to be driven by the low-frequency content. The lower low-frequency noise levels observed upstream, combined with higher annoyance levels than downstream, seem to imply that the low-frequency leading-edge turbulent inflow noise is less important for the annoyance of modern wind turbines than the higher-frequency turbulent-boundary-layer trailing-edge noise.

At the rated wind speed, the sound pressure levels of the NREL wind turbine is approximately 10 dB higher than for the smaller NTK turbine. The difference between the turbines at this wind speed, in terms of SQMs, is relatively smaller. The SQMs decrease less with distance for the NREL turbine than for the NTK turbine. This indicates that the distance to a modern turbine may have to be increased more to achieve a similar decrease in SQM than for an older wind turbine.

The results from a listening experiment showed similar annoyance trends as the numerical results. In general, the larger NREL turbine was perceived as roughly 30% more annoying than the smaller NTK turbine. The decrease in perceived annoyance with distance for the NREL turbine is faster than for the NTK turbine, which is the opposite of all numerical metrics. The annoyance ratings showed a good match with the Zwicker PA metric and with $L_{A,eq}$. The relations between these metrics and the annoyance ratings differ between the turbines, however, which implies that turbine size and mode of operation potentially have an influence on the human perception of wind turbine noise and the related scaling laws.

The next step in this research is to expand the set of input variables to other environmental factors, such as air temperature, pressure, and humidity, and different ground types. Based on the findings by Müller *et al.* [6], specific conditions of high annoyance will be investigated numerically. The difference between up- and downstream annoyance for the NREL turbine at high wind speeds will also be expanded upon with an investigation of the individual contributions of TE and TI noise.

Acknowledgments

We would like to acknowledge and thank the 35 participants in our listening experiment for their voluntary participation. This research would not be possible without them.

The listening experiment results of this paper were made possible by the financial support from the *Blade Extensions for Silent Turbines (BEST)* project (HER+22-02-03415120) which is supported by the Netherlands Enterprise Agency (*Rijksdienst voor Ondernemend Nederland (RVO)*), acting on behalf of the Dutch Ministry of Economic Affairs, using the Renewable Energy Transition subsidy (*subsidie Hernieuwbare Energietransitie* (HER+ 2022-02)), part of the Topsector Energy (TSE) subsidies.

This publication is also part of the *Listen to the future* project (project number 20247), a part of the Veni 2022 research programme (Domain Applied and Engineering Sciences). The latter project is granted to Roberto Merino-Martinez and is (partially) financed by the Dutch Research Council (NWO).

References

[1] J. Lee and F. Zhao, “GWEC Global Wind Report 2024,” Global Wind Energy Council, Brussels, Belgium, Tech. Rep., 2024.

[2] G. Costanzo, G. Brindley, and P. Tardieu, “Wind energy in Europe - 2024 Statistics and the outlook for 2025-2030,” Wind Europe, Brussels, Belgium, Tech. Rep., Feb. 2025.

[3] F. Van Den Berg, E. Koppen, J. Boon, and M. Ekelschot-Smink, “Sound power of onshore wind turbines and its spectral distribution,” *Sound & Vibration*, vol. 59, no. 1, p. 1716, Jan. 2025. DOI: 10.59400/sv1716.

[4] D. S. Michaud, K. Feder, S. E. Keith, *et al.*, “Exposure to wind turbine noise: Perceptual responses and reported health effects,” en, *The Journal of the Acoustical Society of America*, vol. 139, no. 3, pp. 1443–1454, Mar. 2016. DOI: 10.1121/1.4942391.

[5] D. S. Michaud, S. E. Keith, K. Feder, *et al.*, “Personal and situational variables associated with wind turbine noise annoyance,” en, *The Journal of the Acoustical Society of America*, vol. 139, no. 3, pp. 1455–1466, Mar. 2016. DOI: 10.1121/1.4942390.

[6] F. J. Y. Müller, V. Leschinger, G. Hübner, and J. Pohl, “Understanding subjective and situational factors of wind turbine noise annoyance,” en, *Energy Policy*, vol. 173, p. 113 361, Feb. 2023. DOI: 10.1016/j.enpol.2022.113361.

[7] J. L. Davy, K. Burgemeister, and D. Hillman, “Wind turbine sound limits: Current status and recommendations based on mitigating noise annoyance,” *Applied Acoustics*, vol. 140, pp. 288–295, Nov. 2018. DOI: 10.1016/j.apacoust.2018.06.009.

[8] F. Van Den Berg, “Do wind turbines produce significant low frequency sound levels?” In *11th International Meeting on Low Frequency Noise and Vibration and Its Control*, Maastricht, Netherlands, Aug. 2004.

[9] B. Thorne, “The Problems With “Noise Numbers” for Wind Farm Noise Assessment,” en, *Bulletin of Science, Technology & Society*, vol. 31, no. 4, pp. 262–290, Aug. 2011. DOI: 10.1177/0270467611412557.

[10] J. K. Kirkegaard, D. P. Rudolph, S. Nyborg, *et al.*, “Tackling grand challenges in wind energy through a socio-technical perspective,” en, *Nature Energy*, vol. 8, no. 7, pp. 655–664, Jun. 2023. DOI: 10.1038/s41560-023-01266-z.

[11] J. K. Kirkegaard and D. N. Frantzen, “Learning from wind energy controversies: Listening to the noise,” en, *EU Research*, vol. Winter 2024, no. 40, pp. 32–34, 2024.

[12] M. Vorländer, *Auralization: Fundamentals of Acoustics, Modelling, Simulation, Algorithms and Acoustic Virtual Reality* (RWTHedition), en, Second. Cham, Switzerland: Springer International Publishing, 2020, ISBN: 978-3-030-51201-9. DOI: 10.1007/978-3-030-51202-6.

[13] R. Merino-Martínez, R. Pieren, and B. Schäffer, “Holistic approach to wind turbine noise: From blade trailing-edge modifications to annoyance estimation,” en, *Renewable and Sustainable Energy Reviews*, vol. 148, p. 111 285, Sep. 2021. DOI: 10.1016/j.rser.2021.111285.

[14] A. Bresciani, J. Maillard, and L. d. Santana, “Perceptual evaluation of wind turbine noise,” en, in *16ème Congrès Français d’Acoustique, CFA2022*, Marseille, France: Société Française d’Acoustique; Laboratoire de Mécanique et d’Acoustique, Apr. 2022.

[15] J. S. Pockelé, “Auralisation of Modelled Wind Turbine Noise for Psychoacoustic Listening Experiments,” M.S. thesis, Delft University of Technology and Technical University of Denmark, Delft, Netherlands, Oct. 2023.

[16] A. P. C. Bresciani, “Physical and perceptual prediction of wind turbine noise,” English, Doctoral thesis, University of Twente, Twente, Netherlands, Mar. 2024. DOI: 10.3990/1.9789036559546.

[17] F. Bertagnolio, H. A. Madsen, and A. Fischer, “A combined aeroelastic-aeroacoustic model for wind turbine noise: Verification and analysis of field measurements,” en, *Wind Energy*, vol. 20, no. 8, pp. 1331–1348, Aug. 2017. DOI: 10.1002/we.2096.

[18] T. J. Larsen and A. M. Hansen, “How 2 HAWC2, the user’s manual,” DTU, Department of Wind Energy, Roskilde, Denmark, Technical Report Risø-R-1597(ver. 13.0)(EN), May 2023.

[19] R. Parchen, “Progress report DRAW: A prediction scheme for trailing-edge noise based on detailed boundary-layer characteristics,” TNO Institute of Applied Physics, The Netherlands, TNO Report HAG-RPT-980023, 1998.

[20] F. Bertagnolio, A. Fischer, and W. Jun Zhu, “Tuning of turbulent boundary layer anisotropy for improved surface pressure and trailing-edge noise modeling,” en, *Journal of Sound and Vibration*, vol. 333, no. 3, pp. 991–1010, Feb. 2014. DOI: 10.1016/j.jsv.2013.10.008.

[21] R. K. Amiet, “Acoustic radiation from an airfoil in a turbulent stream,” en, *Journal of Sound and Vibration*, vol. 41, no. 4, pp. 407–420, Aug. 1975. DOI: 10.1016/S0022-460X(75)80105-2.

[22] F. Bertagnolio, H. A. Madsen, A. Fischer, and C. Bak, “A semi-empirical airfoil stall noise model based on surface pressure measurements,” en, *Journal of Sound and Vibration*, vol. 387, pp. 127–162, Jan. 2017. DOI: 10.1016/j.jsv.2016.09.033.

[23] T. F. W. Embleton, J. E. Piercy, and G. A. Daigle, “Effective flow resistivity of ground surfaces determined by acoustical measurements,” en, *The Journal of the Acoustical Society of America*, vol. 74, no. 4, pp. 1239–1244, Oct. 1983. DOI: 10.1121/1.390029.

[24] M. Delany and E. Bazley, “Acoustical properties of fibrous absorbent materials,” en, *Applied Acoustics*, vol. 3, no. 2, pp. 105–116, Apr. 1970. DOI: 10.1016/0003-682X(70)90031-9.

[25] Y. Tian and B. Cotté, “Modelling of ground and atmospheric effects on wind turbine noise,” en, Apr. 2015.

[26] International Organisation for Standardisation (ISO), “Acoustics - Attenuation of sound during propagation outdoors - Part 1: Calculation of the absorption of sound by the atmosphere,” Geneva, Switzerland, International Standard ISO 9613-1, Aug. 1993.

[27] H. E. Bass, L. C. Sutherland, A. J. Zuckerwar, D. T. Blackstock, and D. M. Hester, “Atmospheric absorption of sound: Further developments,” en, *The Journal of the Acoustical Society of America*, vol. 97, no. 1, pp. 680–683, Jan. 1995. DOI: 10.1121/1.412989.

[28] F. Bertagnolio, A. Fischer, H. Aagaard Madsen, K. Enevoldsen, P. Hansen, and C. B. M. Pedersen, *NordTank NTK 500/41 Wind Turbine Definition along with Noise and SCADA Measurement Data*, 2024. DOI: 10.11583/DTU.27684813.V1.

[29] F. Bertagnolio, H. A. Madsen, A. Fischer, and C. Bak, “Validation of an Aero-Acoustic Wind Turbine Noise Model Using Advanced Noise Source Measurements of a 500kW Turbine,” en, in *Proceedings of the 16th International Symposium on Transport Phenomena and Dynamics of Rotating Machinery*, Apr. 2016.

[30] J. Jonkman, S. Butterfield, W. Musial, and G. Scott, “Definition of a 5-MW Reference Wind Turbine for Offshore System Development,” en, National Renewable Energy Laboratory (NREL), Golden, CO, USA, Tech. Rep. NREL/TP-500-38060, 947422, Feb. 2009. DOI: 10.2172/947422.

[31] M. Drela, “XFOIL: An Analysis and Design System for Low Reynolds Number Airfoils,” en, in *Low Reynolds Number Aerodynamics*, T. J. Mueller, Ed., ser. Lecture Notes in Engineering, Berlin, Heidelberg: Springer, 1989, pp. 1–12, ISBN: 978-3-642-84010-4. DOI: 10.1007/978-3-642-84010-4_1.

[32] International Organisation for Standardisation (ISO), “Standard Atmosphere,” Geneva, Switzerland, International Standard ISO 2533:1975, May 1975.

[33] Koninklijk Nederlands Meteorologisch Instituut (KNMI), *KNMI - Klimaatviewer*, nl, 2024.

[34] International Electrotechnical Commission (IEC), “Wind turbines - Part 11: Acoustic noise measurement techniques,” en, International Standard IEC 61400-11:2012, Nov. 2012.

[35] J. S. Pockelé and R. Merino-Martinez, “Influence of Ambient Noise in Sound Quality Assessment of Auralised Wind Turbine Noise,” in *11th Edition of the International Conferences on Wind Turbine Noise*, Copenhagen, Denmark, Jun. 2025.

[36] R. Merino-Martínez, R. Pieren, B. Schäffer, and D. G. Simons, “Psychoacoustic model for predicting wind turbine noise annoyance,” en, in *Proceedings of the 24th International Congress on Acoustics*, vol. A11: Psychoacoustics, Gyeongju, Korea, Oct. 2022.

[37] G. F. Greco, R. Merino-Martinez, A. Osses, and S. Langer, “SQAT: A MATLAB-based toolbox for quantitative sound quality analysis,” in *INTER-NOISE and NOISE-CON Congress and Conference Proceedings*, Chiba, Tokyo, Japan, Aug. 2023, pp. 7172–7183. DOI: 10.3397/IN_2023_1075.

[38] International Organisation for Standardisation (ISO), “Acoustics - Methods for calculating loudness – Part 1: Zwicker method,” Geneva, Switzerland, International Standard ISO 532-1:2017, 2017.

[39] G. Von Bismarck, “Sharpness as an attribute of the timbre of steady sounds,” *Acta Acustica united with Acustica*, vol. 30, no. 3, pp. 159–172, 1974.

[40] P. Daniel and R. Weber, “Psychoacoustical Roughness: Implementation of an Optimized Model,” *Acta Acustica united with Acustica*, vol. 83, no. 1, pp. 113–123, Jan. 1997.

[41] A. Osses, R. García León, and A. Kohlrausch, “Modelling the sensation of fluctuation strength,” *Proceedings of Meetings on Acoustics*, vol. 28, no. 1, p. 050 005, Sep. 2016. DOI: 10.1121/2.0000410.

[42] H. Fastl and E. Zwicker, *Psychoacoustics: facts and models* (Springer series in information sciences 22), en, 3rd. Berlin , Germany; New York, NY, USA: Springer, 2007, ISBN: 978-3-540-23159-2.

[43] G. F. Greco, R. Merino-Martínez, and A. Osses, *SQAT: A sound quality analysis toolbox for MATLAB*, v1.2. Zenodo. DOI: 10.5281/ZENODO.14641811, Jan. 2025.

[44] R. Merino-Martínez, R. M. Yupa-Villanueva, B. von den Hoff, and J. S. Pockelé, “Human response to the flyover noise of different types of drones recorded in field measurements,” in *3rd Quiet Drones conference*, Manchester, UK, Sep. 2024.

[45] J. S. Pockelé and R. Merino-Martínez, “Pyschoacoustic Evaluation of Modelled Wind Turbine Noise,” English, in *Proceedings of the 30th International Congress on Sound and Vibration*, Amsterdam, Netherlands: The International Institute of Acoustics and Vibration, Jul. 2024.

[46] J. Vos and M. M. J. Houben, “Annoyance caused by the low-frequency sound produced by aircraft during takeoff,” *The Journal of the Acoustical Society of America*, vol. 152, no. 6, pp. 3706–3715, Dec. 2022, ISSN: 0001-4966. DOI: 10.1121/10.0016596.

[47] M. P. Norton and D. G. Karczub, *Fundamentals of Noise and Vibration Analysis for Engineers*. Cambridge, UK: Cambridge University Press, 2003, ISBN: 978-0-511-67173-9.

[48] S. Oerlemans, M. Fisher, T. Maeder, and K. Kögler, “Reduction of Wind Turbine Noise Using Optimized Airfoils and Trailing-Edge Serrations,” en, *AIAA Journal*, vol. 47, no. 6, pp. 1470–1481, Jun. 2009. DOI: 10.2514/1.38888.

[49] R. Merino-Martínez, B. von den Hoff, and D. G. Simons, “Design and Acoustic Characterization of a Psycho-acoustic listening facility,” English, in *Proceedings of the 29th international congress on sound and vibration*, E. Carletti, Ed., Prague, Czech Republic: IIAV CZECH s.r.o., Jul. 2023, pp. 274–281, ISBN: 978-80-11-03423-8.

[50] J. S. Pockelé, *Graphical User Interface for the Psychoacoustic Listening Laboratory (PALILA GUI)*, v1.2.0. Zenodo., Mar. 2025. DOI: 10.5281/ZENODO.15100497.